UNIVERSITÀ DEGLI STUDI DI TORINO

DEPARTMENT OF MEDICAL SCIENCES

Master's Degree in Medical Biotechnology

MASTER THESIS

Class LM-9

Diacylglycerol kinase alpha promotes ubiquitination and cell surface downregulation of chimeric antigen receptor

Supervisor:
Prof. Andrea Graziani

Candidate:
Alessia Labate

Co-supervisor:
Dr. Valeria Malacarne

Student ID:
1034012

Università di Torino

Molecular Biotechnology Center

Academic Year: 2022-2023

Contents

Abstract

Loss of chimeric antigen receptor (CAR) surface expression emerged as a key determinant in CAR-T cell dysfunction. However, the underlying mechanisms directing CAR trafficking remain largely unknown. Current strategies to enhance the anti-tumour effectiveness of CAR-T cells involve targeting of negative regulators of T cell signalling, such as diacylglycerol kinase α (DGKα), which inhibit diacylglycerol (DAG)-driven TCR signalling by converting DAG to phosphatidic acid (PA). Although it is widely accepted that its kinase activity does play a role in limiting CAR-T cell function, several evidence suggest that it may act more upstream in the TCR signalling. Here, we showed that in DGKα depleted CAR-T cells, the engagement of tumour antigen result in a reduced loss of CARs from the cell surface compared to WT CAR-T cells. Reconstitution with both DGKα WT or kinase dead (KD) mutant reduced the amount of the receptor at the cell surface, suggesting a new kinase-independent function of DGKα in CAR regulation. Once internalized, CAR is saved from antigen-induced lysosomal degradation in DGKα KO CAR-T cells, due to a reduction of the E3 ubiquitin ligase Cbl recruitment to the receptor, and rather recycled back to the plasma membrane. Thus, DGKα is responsible for CAR ubiquitination, degradation and finally for the reduction of the CAR at the cell surface upon antigen stimulation. Together, these data indicate that DGKα couples antigen-induced T cell activation to the triggering of the negative feedback mechanism that lead to lysosomal degradation of the activated CAR.

Introduction

T Cell Receptor signalling and fate

T cells play a central role in the adaptive immune response, undergoing activation through the binding of the T cell receptor (TCR) to antigens, presented on major histocompatibility complex (MHC) molecules by antigen-presenting cells (APCs) (Dong et al., 2019); this type of cellular interaction allows the formation of the immunological synapse, characterized by a polarized increase in diacylglycerol (DAG) at the contact area between the two cell types (Dustin et al., 2010). This process is crucial for effective antigen recognition.

TCR is a cell-surface protein complex consisting in several subunits that work together and organized in six polypeptides: the highly variable TCRα and TCRβ chains are responsible for antigen recognition; the invariant heterodimers CD3ε-CD3δ and CD3ε-CD3γ, together with the CD3ζ-CD3ζ homodimer, are responsible for converting antigen recognition to intracellular signal transduction (Mariuzza et al., 2020).

The CD3 chains contain immunoreceptor tyrosine-based activation motifs (ITAMs), with CD3γ, δ, and ε each containing one ITAM, and the ζ chains each having three ITAMs. TCR signalling is initiated when these ITAMs are phosphorylated by the Src family kinases (Lck and Fyn) at tyrosine residues which become accessible to Lck only after stimulation (Brownlie et al., 2013).

Once phosphorylated, ITAMs of the ζ chain recruit and bind Zap-70 (ζ-chain-associated protein kinase of 70 kDa) which in turn induces the phosphorylation of the linker of activated T cells (LAT) (Brownlie et al., 2013); phosphorylated LAT recruits phospholipase C-γ (PLCγ) (Wu et al., 2020) leading to the hydrolysis of phosphatidylinositol 4,5-bisphosphate (PIP2) into DAG and inositol 1,4,5-triphosphate (IP3) (Krishna and Zhong, 2013), two important second messengers that mediate the downstream effector functions.

The amount of the TCR exposed at the cell surface is essential for the proper regulation of the T cell signalling and ultimately of the T cell function (Geisler, et al., 2004; Smith-Garvin et al., 2009).

TCR trafficking is regulated by multiple processes: de novo synthesis, transport of newly assembled receptors, endocytosis of surface TCRs, recycling to the plasma membrane of internalized receptors, and receptor degradation (Onnis and Baldari, 2019). Specifically, the internalization of the TCR occurs both in a clathrin-dependent and independent manner (Capitani and Baldari, 2021). Following internalization, TCR complexes are compartmentalized into early endosomes, which are further fused in $Rab5^{+}$ sorting endosomes; from here, they can be sorted

into Rab6^{+} vesicles for the retrograde transport to the trans-Golgi network or in Rab4 (short-loop, fast cycle) or Rab11 (long-loop, short cycle) positive compartment for recycling. Finally, TCR may be directed into Rab7^{+} late endosomes for lysosomal degradation (Fig. 1).

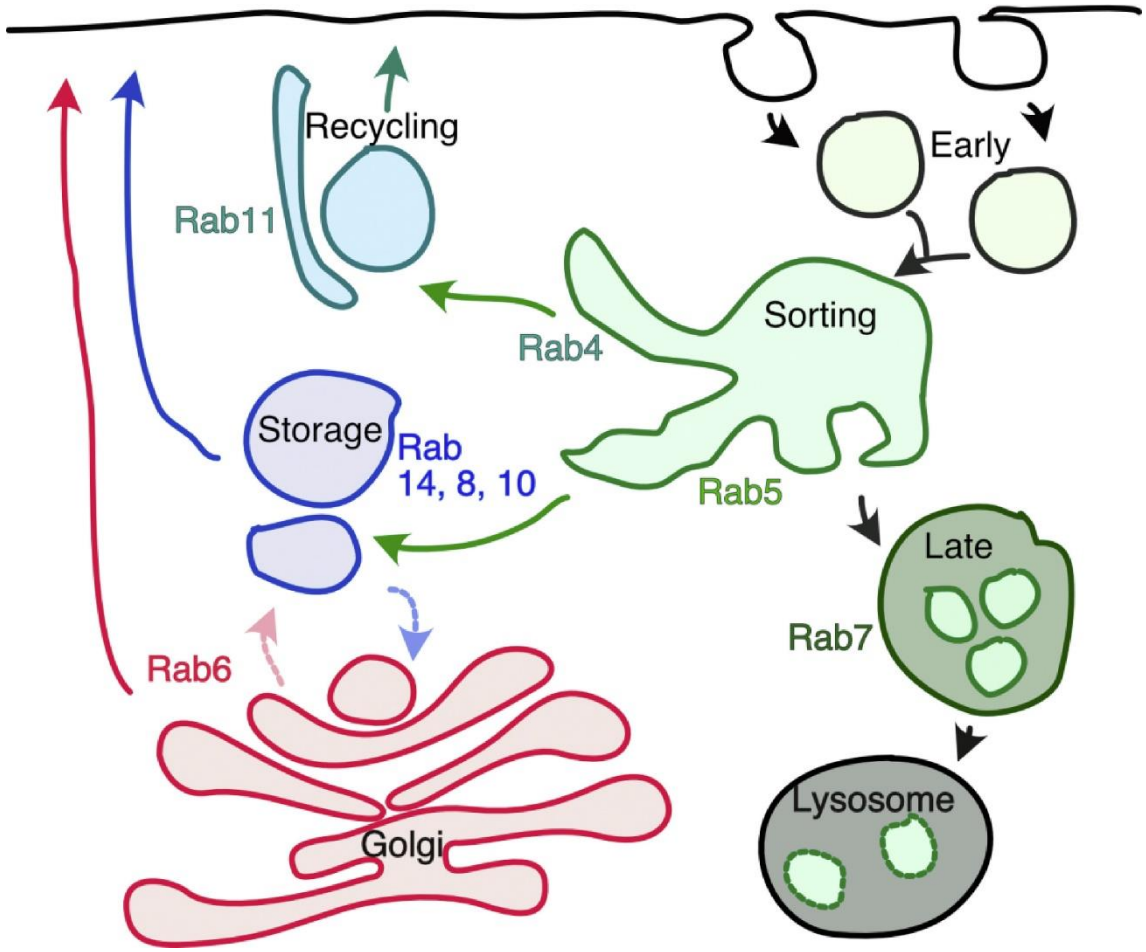

FIGURE 1. Overview of endosomal transport: Plasma membrane-derived vesicles traffic towards the plasma membrane, forming a network of endosomal compartments. First TCR is directed towards early endosomes that fuse with sorting endosome (Rab5^{+}). Here, cargos are selected for various destinations: lysosomal degradation (Rab7^{+}), retrograde transport to the trans-Golgi network (Rab6^{+}), or recycling. Constitutive recycling can occur rapidly (mediated by Rab4) or slowly (driven by Rab11), while antigen-induced recycling (involving Rab14, 8, and 10) is initially slow under normal conditions but can be modulated by specific cellular signalling pathways (Adapted from Evnouchidou et al., 2022).

Ubiquitination as a critical regulator of TCR abundance on the t cell surface

Ubiquitination is a post-translational modification that alters the stability, protein-protein interactions, enzymatic action and cellular localization of the targeted protein (Acconcia et al., 2009). It's involved in regulating a wide range of cellular processes, including signal transduction and protein trafficking (Mukhopadhyay et al., 2007), by the addition of a highly conserved 76 aminoacid (8kDa, ubiquitin) in a target protein.

Ubiquitination reactions are catalysed by three classes of enzymes (E1, E2 and E3), resulting in the formation of a covalent bond between ubiquitin and a lysine (Lys) residue in the target protein (Acconcia et al., 2009). The specificity of these effects is determined by the diverse abilities of E3 ligases to promote different types of protein ubiquitination (Thien et al., 2005). Among the E3 ubiquitin ligases, c-CBL and Cbl-b (belonging to the Cbl (Casitas B-lymphoma) family proteins) are known negative regulators of TCR signal transduction highly expressed in T cells (Naramura et al., 2002; Gavali et al., 2021). Indeed, by targeting multiple T cell signalling proteins to the lysosome for degradation, they are responsible for switching off TCR signalling (Sitaram et al., 2019). While Cbl-b mostly target intracellular proteins involved in TCR signalling, such as PI3K, Vav1 and PLCγ, c-Cbl primary limits T cell activation by binding to the TCR CD3ζ chain via ZAP70, thus leading to the receptor ubiquitination and consequent loss of the receptor from the cell surface (Liu et al., 2002). Consistently with a signal reduction following Cbl-mediated TCR ubiquitination, T cells derived from c-Cbl and Cbl-b double KO are hyper responsive upon anti-CD3 stimulation (Naramura et al., 2002).

Chimeric Antigen Receptor - T cells: limitation and potential strategies

Among the adoptive T cell therapies, chimeric antigen receptor (CAR) T cells are considered a revolutionary and successful frontier in cancer treatment (Sterner et al., 2021). CARs are composed of an antibody fragment (scFv) designed to recognize specific antigens, an hinge region serving as the extracellular link to the transmembrane domain, a transmembrane domain, and an intracellular signalling domain, composed by the CD3ζ chains of the T-cell receptor (Sterner et al., 2021; Jackson, H et al., 2016). Furthermore, based on the generation of CARs, it may incorporate a co-stimulatory domain such as CD28, 4-1BB or both (Fig.2)

The recognition of the antigen expressed on the cell surface of the target cells enabled MHC-independent target recognition by T cells and results in strong T-cell activation and accordingly robust antitumour response (Sterner et al., 2021).

CAR-T therapy have demonstrated excellent results so far, especially in treating haematological malignancies. However, they still feature several limitations, mostly due to different mechanisms of resistance such as tumour-intrinsic mechanisms allowing immune evasion (i.e. antigen loss or lineage switch), the establishment of an immunosuppressive tumour microenvironment (TME) and CAR-T cell dysfunction itself leading to exhaustion. CAR-T cell exhaustion is characterized by a reduction in time of T cell effector functions and is determined by prolonged stimulation with the antigen and/or tonic signalling, namely, spontaneous activation of the CAR in the absence of the tumour antigen (Ruella et al., 2023). Altogether, these processes limit the *in vivo* persistence of CAR-T cells. Many intervention has been proposed to overcome CAR-T cell dysfunction, such as targeting of inhibitory receptor (i.e. Cytotoxic T-Lymphocyte-Associated Protein 4 (CTLA-4), Programmed Cell Death Protein 1 (PD-1)) or negative regulator of T cell signalling (such as diacylglycerol kinases (DGKs), ubiquitin ligases and phosphatases), as well as metabolic reprogramming of CAR-T cells towards a memory and persistent phenotype.

Interestingly, several recent studies have contributed to identifying reduced exposure of the CAR receptor on the cell membrane as one of the events leading to CAR-T cells dysfunction (Davenport et al., 2015; Eyquem et al., 2017; Walker et al., 2017, Li et al., 2020, Agarwal et al., 2023). In fact, following repeated antigen-receptor interactions, the effectiveness of CAR-T cells decreases due to the downregulation of the CAR (Davenport et al., 2015). This downregulation is caused by the lysosomal degradation of the receptor following its rapid ubiquitination upon encountering the antigen (Li et al., 2020). For instance, an effective strategy to regulate CAR expression and

trafficking (compared to CAR-T cells produced using lentiviral or retroviral vectors) is the integration of the CAR gene into the locus of the constant region of the TCR alpha chain (TRAC). This strategy resulted in a more physiologically regulated internalization and re-expression of the CAR receptor following antigen stimulation, improving anti-tumour activity in haematological malignancies (Eyquem et al., 2017). Recent studies have shown that CAR-T cells knockout for the inhibitory receptor CTLA-4 are more efficient in killing the target tumour, as long as the CAR stay high at the cell surface (Agarwal et al., 2023). Together, these results suggest that maintaining high expression levels of the CAR at the cell surface by limiting CAR internalization and degradation may be an excellent strategy to achieve superior antitumour efficacy.

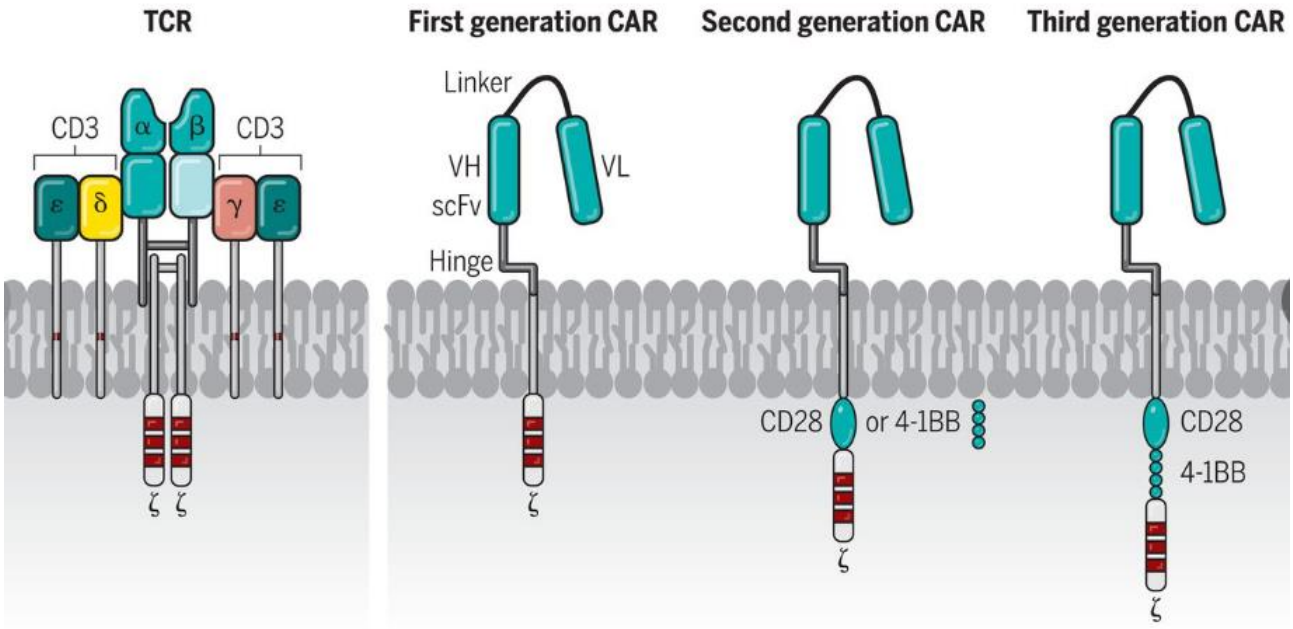

June CH et al., CAR T cell immunotherapy for human cancer. Science. 2018

FIGURE 2. COMPARISON BETWEEN TCR and CAR STRUCTURE: The TCR is a protein complex expressed on the surface of T cells, consisting of αβ heterodimers, which confer specificity to antigens, and two CD3ε, a CDδ, a CD3γ, and a CD3ζ homodimer. CARs (First Generation) are composed of an antigen-binding domain that imparts antigenic specificity, derived from the variable heavy (VH) and light (VL) chains of monoclonal antibodies, linked by a linker to form a single-chain variable fragment (scFv); the hinge domain serves as the region connecting the extracellular domain to the transmembrane domain; the intracellular domain comprises the CD3ζ chain of the TCR, essential for the propagation of antigen-induced intracellular signalling. Second-Generation CARs additionally feature a CD28 or 41BB costimulatory domain. Third-Generation CARs express both the CD28 and 41BB costimulatory domains simultaneously (Adapted from June et al., 2018).

DGKα as negative regulator in TCR signalling

Diacylglycerol kinases (DGKs) are a class of lipid kinases responsible for catalyzing the phosphorylation of diacylglycerol (DAG) to generate phosphatidic acid (PA) (Zhong et al., 2008, Arranz-Nicolás et al., 2019). DGKα and DGKζ, the two main isoforms of diacylglycerol kinases (DGKs) expressed by T lymphocytes, are considered as the primary inhibitors of diacylglycerol (DAG) function. Although there is some overlap in their function, they are not entirely redundant: while DGKζ is responsible for the phosphorylation of most of the DAG produced by PIP2 hydrolysis upon TCR-stimulation, DGKα is known to control a small pool of DAG enriched at the immune synapse (Ruffo et al., 2016).

DGKα and DGKζ are highly expressed in naïve T cells, and their expression, as well as their activity, decreases in activated T cells (Merida et al., 2009; Baldanzi et al., 2011). This leads to enhanced DAG-mediated signalling (Baldanzi et al., 2011). Consequently, DGKs induction mediates a hypo functional and tolerogenic antigen-induced T cell state known as T cell anergy (Olenchock et al., 2006), making DGKs negative regulators of T cells. The anergic state of T lymphocytes can be considered a mechanism of tumour immune escape. It involves the development of peripheral tolerance, where lymphocytes do not become activated and fail to produce IL-2 for proliferation in response to antigenic stimuli (Joshi et al., 2013).

Interestingly, genome-wide CRISPR screening in CD8+ human T cells and a pooled short hairpin RNA (shRNA) screening in a mouse melanoma model in vivo identified DGKα and DGKζ as inhibitors of T cell receptor signalling (Shifrut et al., 2018; Zhou et al., 2014).

Thus, the overexpression of DGKα in T cells mimics an anergic state characterized by reduced Ras activation, a protein involved in cell proliferation, differentiation, and survival; on the contrary, the deletion of DGKα or DGKζ in primary cells results in cellular resistance to anergy (Olenchock etal., 2006). The notion that DGKα or ζ KO promotes T cell activation has contributed to the hypothesis that eliminating these molecules may also enhance the T cell response to tumours(Kureshi et al., 2023) and it has been demonstrated that a dual DGKα/ζ inhibitor (DGKi) reduce the activation threshold required to induce TCR signalling in effector T cells (Kureshi et al., 2023).

Several studies have found enrichment in DGKα expression in tumour-infiltrating lymphocytes (TILs) in human patients with renal cell cancer and xenograft mouse models (Lee, et al., 2018).

Consistently with the role of negative regulator of T cell function with an enhanced expression in

tumour-infiltrating T cells, an increasing body of evidence indicate that DGKα targeting enhances efficacy of both adoptive T cell therapies.

It has been shown that dual targeting of DGKα and DGKζ in CAR-T cells enhances the cytotoxic activity and the antitumour effect in a xenograft mouse model of glioblastoma by opposing to the TGFβ and prostaglandin E2 enriched immunosuppressive microenvironment (Jung et al., 2018). Moreover, pharmacological inhibition of DGKα in CD8+ CTLs infiltrating human renal cancer rescues TCR distal signalling in CTLs infiltrating in human renal cancer (Prinz et al., 2012) and enhance efficacy of anti-PD-1 treatment in B16 melanoma, MC38 colon cancer and LLC lung cancer murine models (Fu et al., 2021). Finally, CAR-T cells from either DGKα -/- or DGKζ -/- mice feature enhanced anti-tumour activity and enhanced persistence in murine models of mesothelioma and lung cancer (Riese et al., 2013).

Although it is assumed that inhibiting DGKs (ζ and α) improves T cell function by enhancing DAG signalling, cytokine release, and ultimately tumour cell killing, none of these studies have investigated which mechanisms is responsible for the beneficial effects of targeting DGKs in adoptive T cell therapies. However, the deletion of DGKζ leads to increased Ras/ERK activation and enhanced recruitment downstream of the T-cell receptor and co-stimulation (Ávila-Flores et al., 2017), while DGKα does not (Joshi et al., 2013). DGKα is rather responsible for phosphorylating a small pool of DAG at the immunological synapse (Chauveau et al., 2014), suggesting that DGKα may be involved in another as yet unexplored mechanism.

Preliminary results from our laboratory demonstrate that in a model of hypofunctional T cells, characterized by low TCR at the cell surface, DGKα silencing is sufficient to restabish the TCR levels at plasma membrane. Given that CAR share the CD3ζ subunit with the TCR, in this thesis we investigated the hypothesis that DGKα deletion may improve CAR-T cell function by increasing CAR availability at the cell surface.

Results

Cloning OST-DGKα wild type (WT) and kinase dead mutant (KD)

The experimental models present in this study were generated and designed to investigate the role of the DGKα protein in modulating CAR expression on the cell surface.

In particular, we used a second generation CAR with a single-chain variable fragment (scFv) specifically engineered to recognize and bind CD19, an antigen highly expressed on malignant B cells. Within the intracellular domain, the CAR incorporates the co-stimulatory domain CD28 and the CD3ζ subunit of the TCR, responsible for the signal transduction (Fig.). This CAR, namely 19.28ζ, was further engineered by adding a Myc-tag at the N-terminal, thus allowing us to easily detect the receptor (Li et al., 2020).

The initial phase of the project aimed to generate in vitro cellular models that overexpressed an OST-tagged version of DGKα WT (wild type) or DGKα KD (kinase dead) proteins in 19.28ζ Jurkat cells that do or do not express the endogenous DGKα (WT vs DGKα KO, previously generated in the lab) (Fig.3a). The KD mutant is characterized by a mutation in the kinase domain that results in the loss of DGKα kinase activity, thus making it useful for studying its scaffold function (Cutrupi S. et al, 2000).

The coding sequences for OST-DGKα WT and OST-DGKα KD were subcloned into the bicistronic vector CD19-CAR.28ζ H (PGK) eGFP (mCMV) (Recipient Plasmid) that allowed the simultaneous expression of our protein of interest and eGFP (Enhanced Green Fluorescent Protein), thus allowing the subsequent sorting of DGKα+/eGFP+ cells. (Fig.3b)

From the original Recipient Plasmid, the sequence encoding for CD19-CAR.28ζ was removed through enzymatic digestions and replaced with the human DNA sequence of OST-DGKα WT or the mutated KD variant derived from a Donor Plasmid (pUC57-Mini) (Fig.3b).

Briefly, the Recipient Plasmid, 9826 bp in size, was cut with two different restriction enzymes, RsrII and SalI, yielding two fragments: the first 8385 bp (representing the vector) and the second 1441 bp (representing the CAR insert) (Fig.3c). Simultaneously, the pUC57-Mini vectors (one for OST-DGKα WT and one for OST-DGKα KD) were digested with the same restriction enzymes (Fig.3c), generating the two inserts of interest with sticky ends. Subsequently, both OST-DGKα WT

and KD isolated inserts were ligated within the excised Recipient Plasmid (8385 bp) and the cloning was verified by Sanger sequencing (Fig.3d). In order to test the efficiency of the newly produced constructs, 293T cells were transiently transfected. This approach clearly demonstrates the increase in DGKα protein expression compared to the endogenous protein (Fig.3e).

a)

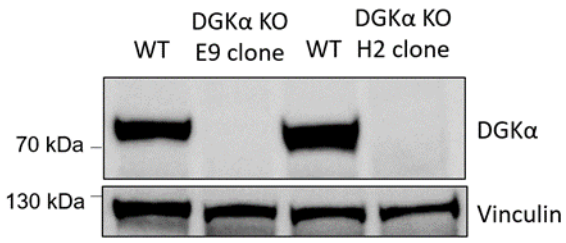

b)

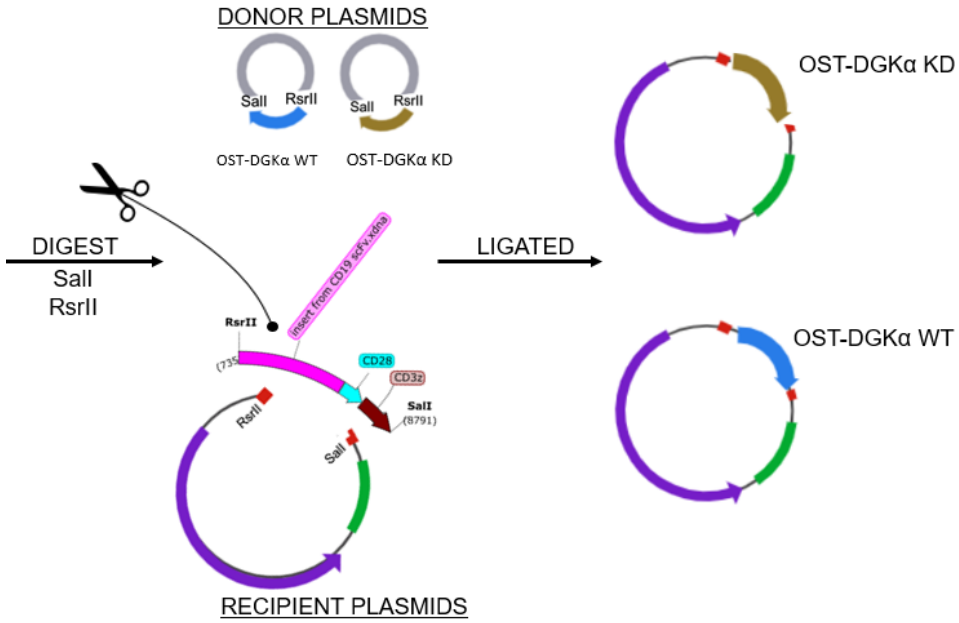

c)

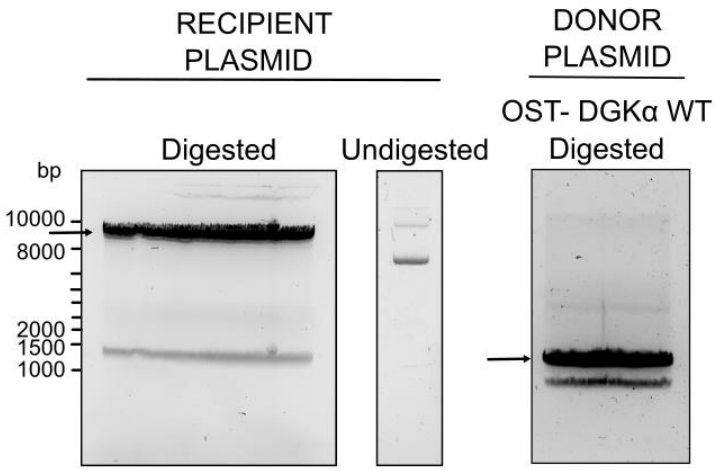

d)

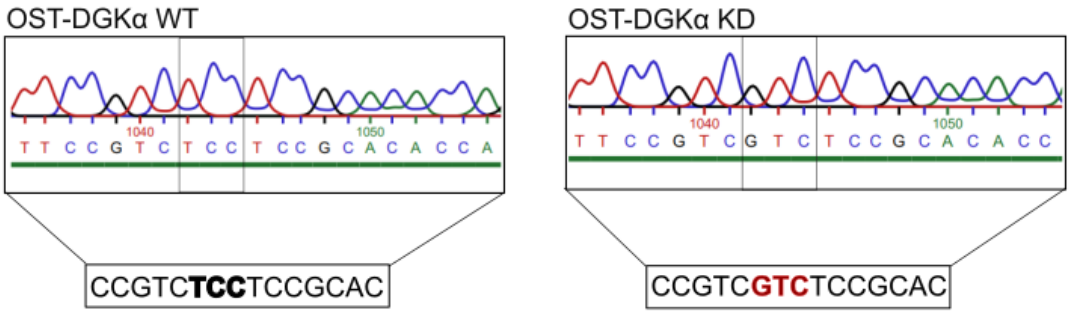

e)

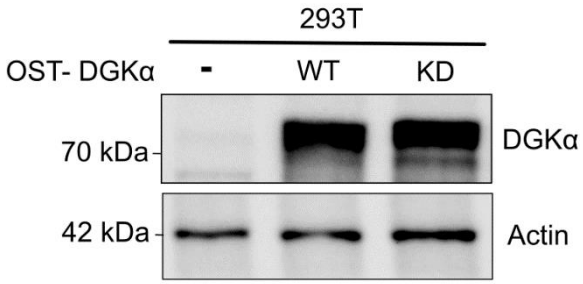

Figure 3. Cloning OST-DGKα WT and OST-DGKα KD constructs: **(a)** Representative blot of Jurkat WT and DGKα KO (E9 and H2 clones) cell lines, previously generated in our laboratory. **(b)** Schematic representation of Donor and Recipient Plasmid digestion with RsrII and SalI restriction enzymes in order to create OST-DGKα WT and OST-DGKα KD vectors for overexpression of the DGKα protein. **(c)** Representative electrophoretic run of the enzymatic digestion of the Recipient Plasmid (left) and Donor Plasmid (right). The arrows indicate which digestion products were extracted from the gel and subsequently ligated as is indicated in the materials and methods. **(d)** Representative Sanger sequencing of the newly generated inserts. The figure shows the mutated triplet (highlighted in red) of DGKα KD variant. **(e)** Representative blot of endogenous DGKα and OST-DGKα protein expression in transiently transfected 293T cells.

Lentiviral transduction and cell sorting

Lentiviral transduction is a widespread practice utilized to introduce the desired gene into cells of interest. This method relies on the ability of lentiviral vectors to infect different cell types and integrate genetic material into the genome of target cells (Roman P. Labbé et al., 2021).

In this thesis work, Jurkat WT and DGKα KO cells were sequentially transduced with CAR and OST-DGKα WT or OST- DGKα KD constructs and double positive cells were sorted. Thus, we generated six cell lines with comparable transduction efficiency of all the constructs (Fig.4a). The overexpression of OST-DGKα WT and KD proteins compared to the endogenous one was also evident (Fig.4b).

In order to confirm that the transduction efficiency was comparable among the different cell lines, we evaluated the protein expression and the transcript levels of 19.28ζ into cells. Western blot and qPCR analysis of CAR mRNA expression did not reveal any significant differences (Fig.4b, c).

Moreover, with the aim of generating a physiological in vitro system for CAR-T cells stimulation, we transduced K562 myelogenous leukemia cells with the CD19 antigen, which is recognized by 19.28ζ CAR-T cells. (Fig.4d). After transduction, cells were sorted to separate K562 cells expressing the tumour antigen from the negative one (Fig.4e). These cell populations have been used in subsequent experiments to stimulate (K562 $CD19^{+}$) or not (K562 $CD19^{-}$) the 19.28ζ CAR-T cells.

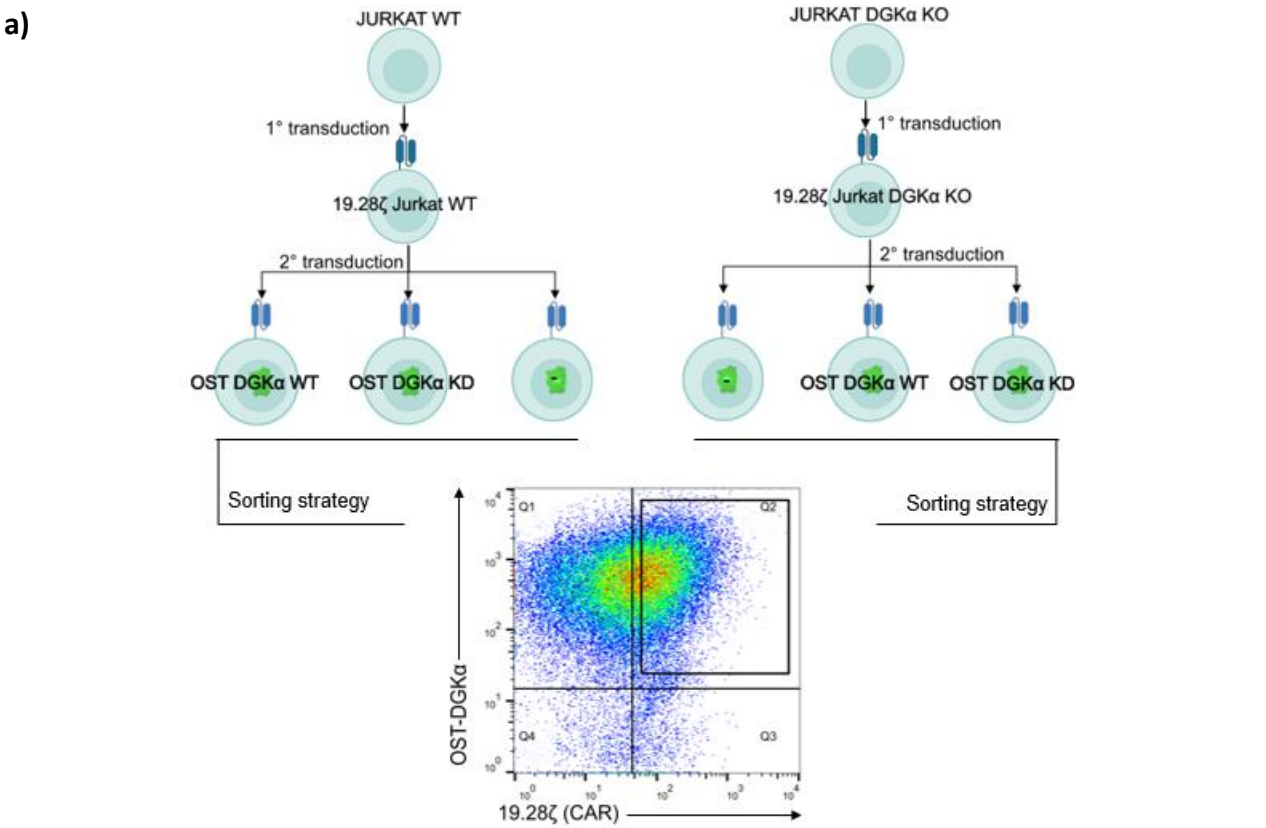
a)
JURKAT WT
1° transduction
19.28ζ Jurkat WT
2° transduction
OST DGKα WT
OST DGKα KD
-
JURKAT DGKα KO
1° transduction
19.28ζ Jurkat DGKα KO
2° transduction
-
OST DGKα WT
OST DGKα KD
Sorting strategy
Sorting strategy
Q1
Q2
Q3
Q4
OST-DGKα
19.28ζ (CAR)

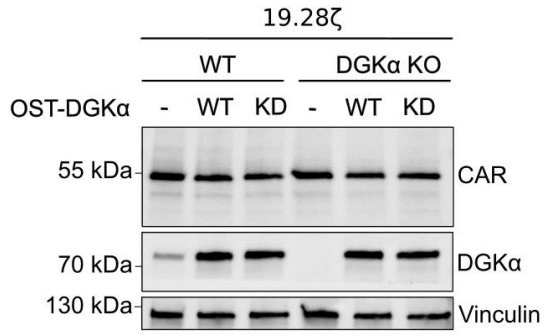
b)
19.28ζ
WT
DGKα KO
OST-DGKα
-
WT
KD
-
WT
KD
55 kDa
CAR
70 kDa
DGKα
130 kDa
Vinculin

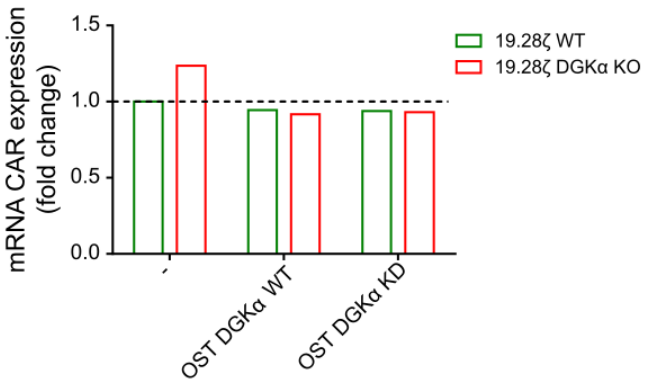
c)
mRNA CAR expression (fold change)
1.5
1.0
0.5
0.0
19.28ζ WT
19.28ζ DGKα KO
-
OST DGKα WT
OST DGKα KD

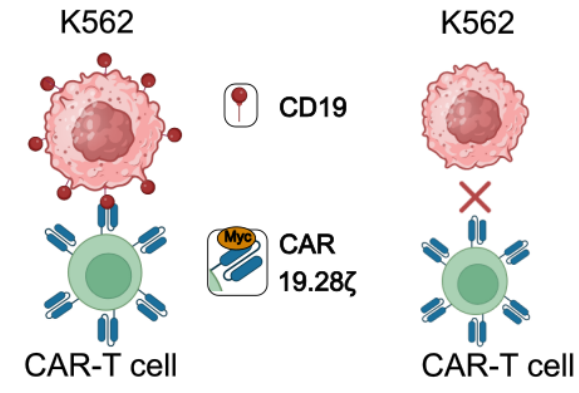
d)
K562
CD19
Myc
CAR
19.28ζ
CAR-T cell
K562
CAR-T cell

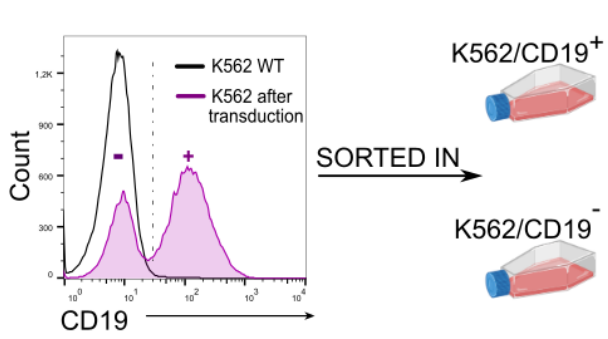
e)
K562 WT
K562 after transduction
Count
-
+
CD19
SORTED IN
K562/CD19+
K562/CD19-

Figure 4. Lentiviral transduction and cell sorting: (a) Transduction and sorting workflow for the generation of the six 19.28ζ Jurkat cell lines. **(b)** Representative blot of CAR and DGKα protein expression levels after transduction. **(c)** mRNA expression level of CAR in all 19.28ζ Jurkat cell lines. **(d)** Cartoon showing the *in vitro* model of CAR-T cells stimulation. Only K562/CD19^{+} cells bind the CAR and induce stimulation in 19.28ζ Jurkat cells. **(e)** Schematic representation of K562/CD19^{+} and CD19^{-} cell lines generation by sorting.

CAR downmodulation requires DGKα

CAR-T cells exhibited various limitations associated with CAR downregulation; specifically, persistent antigen exposure or high tumour burden cause a decrease in receptor surface exposure, resulting in a poor anti-tumoural response (Agarwal et al., 2023). Therefore, dissecting the mechanisms that regulate the amount of CAR exposed to the cell surface may represent a good strategy to ameliorate CAR-T cell effector function. Based on our previous results (see Introduction), we hypothesized that DGKα deletion via CRISPR/Cas9 could prevent the loss of CAR from the cell surface upon CD19 recognition on antigen-expressing cells.

Therefore, we co-cultured 19.28ζ Jurkat with K562/CD19^{+} or K562/CD19^{-} for 1 hour in 1:1 ratio (Fig.4d) to investigate the receptor persistence at the cell surface after tumour antigen encounter. CAR loss was measured through flow cytometry analysis by subtracting the amount of the receptor on the surface under basal conditions (19.28ζ Jurkat co-incubated with K562/CD19^{-}) from the amount of the one after antigen exposure (19.28ζ Jurkat co-incubated with K562/CD19^{+}). The results indicate a higher percentage of CAR loss in 19.28ζ WT cells compared to 19.28ζ DGKα KO cells (Fig.5a). When we reintroduced OST-DGKα WT in 19.28ζ Jurkat DGKα KO, CAR surface protein levels were restored similarly to 19.28ζ Jurkat cells expressing endogenous DGKα, highlighting a specific function of DGKα in driving CAR loss from the cell surface. Surprisingly, this effect was kinase independent since the KD mutant behave exactly as DGKα WT (Fig.5a). Interestingly, the overexpression of both DGKα WT and KD per se (in 19.28ζ WT cells) increased surface CAR loss, indicating that the levels of DGKα are crucial for the regulation of CAR downmodulation (Fig.5a)

In order to exclude effects related to the clonal origin of our 19.28ζ Jurkat DGKα KO cell lines, we repeated the experiment by using a second clone (namely H2) and we confirmed our previous findings (Fig. 5b).

Altogether, these data suggest that DGKα contributes to the CAR loss from the cell surface upon antigen stimulation in a kinase independent manner.

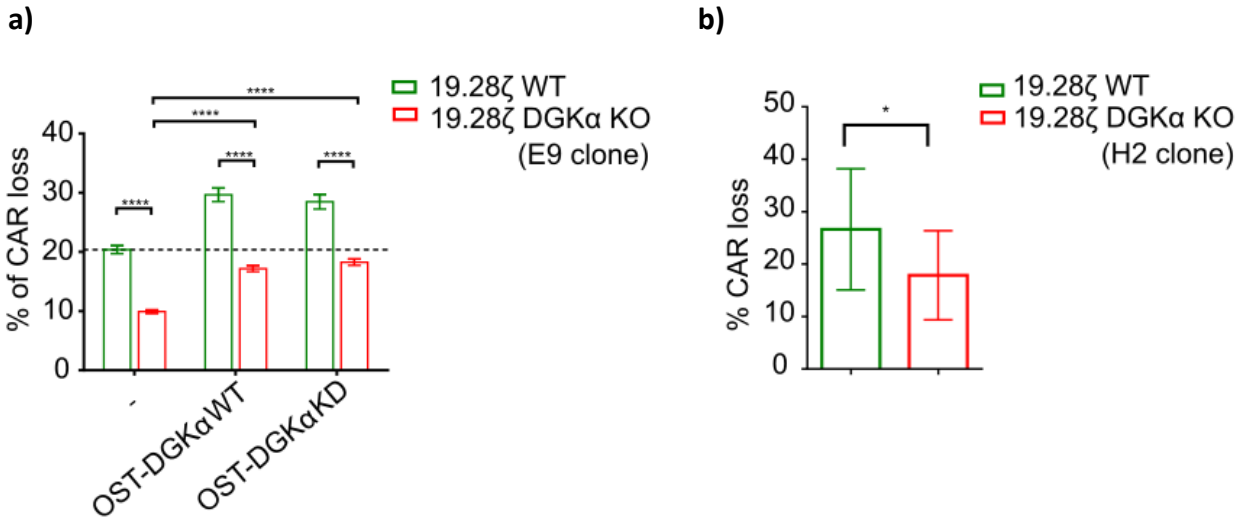

Figure 5. CAR downmodulation after antigen *stimulus:* CAR loss quantification by FACS analysis was calculated by subtracting the quantity of unstimulated receptor (19.28ζ Jurkat co-coltured with K562/CD19^{-}) from the quantity of receptor remaining on the surface after stimulation (19.28ζ Jurkat co-coltured with K562/CD19$^{+)}$.

(a) CAR loss quantification in E9 clone. n= 4 independent experiments, data are mean ± SEM; two-way ANOVA, uncorrected Fisher's LSD multiple comparisons test: **** p< 0.0001.

(b) CAR loss quantification in H2 clone. n=8 independent experiment; data are mean ± SEM; paired t-test * < 0.05.

DGKα deletion promotes CAR recycling to the plasma membrane and prevents CAR degradation

The different percentage of CAR loss from the cell surface that we observed between WT and Knockout (DGKα KO) cells upon tumor antigen interaction, prompted us to investigate the mechanism processes that lead to total receptor downmodulation on the cell surface. These processes include internalization, recycling, and degradation (Fig.1).

Indeed, the inhibition of CAR downmodulation in DGKα KO CAR-T cells could be due to either impaired CAR endocytosis or enhanced recycling of the internalized CAR to the cell surface. Therefore, we assessed both the internalization and recycling rate of CAR in 19.28ζ Jurkat WT or DGKα KO cells according to the scheme showed in methods (Fig.8, 9).

Interestingly, we observed that DGKα deletion per se increased CAR receptor at steady state (Fig.6a), while did not have any significant difference in CAR internalization (Fig.6b). Notably, recycling rate appeared to be significantly increased in cells without DGKα (Fig.6c).

However, the enhanced CAR recycling rate could relay either from a direct impact on the recycling process itself (i.e. DGKα may regulates Rabs, VAMPs or other proteins involved in receptor recycling (Onnis and Baldari, 2019)), or from increased availability of receptors upon internalization since degradation is prevented.

In order to discern between these two possibilities, we first measured CAR degradation, since it was recently demonstrated that engagement of tumor antigens induces strong CAR downmodulation and lysosomal degradation (Li et al., 2020).

We co-cultured 19.28ζ Jurkat WT and DGKα KO cells with K562/CD19^{+} and CD19^{-} cells at 1:1 ratio in the presence of cycloheximide (CHX), a protein synthesis inhibitor, and we monitor CAR degradation (either antigen-induced or not) at various time points (0, 3, 6, and 9 hours). In line with published data, upon engagement with the CD19 tumor target we observed a drastic degradation of CAR in 19.28ζ Jurkat WT cells, which was significantly delayed in 19.28ζ Jurkat DGKα KO (Fig.6d about 92% loss in WT vs 82% loss in DGKα KO after 9h of CHX treatment). Interestingly, even under unstimulated conditions, we measured about 79 % of CAR degradation loss in Jurkat 19.28ζ WT cells compared to 59 % in 19.28ζ Jurkat DGKα KO cells (Fig. 6e).

Collectively, these data strongly support the hypothesis that, in DGKα KO CAR-T cells, the CAR is saved from lysosomal degradation and redirected towards the cell surface upon internalization, whether stimulated by the antigen or not.

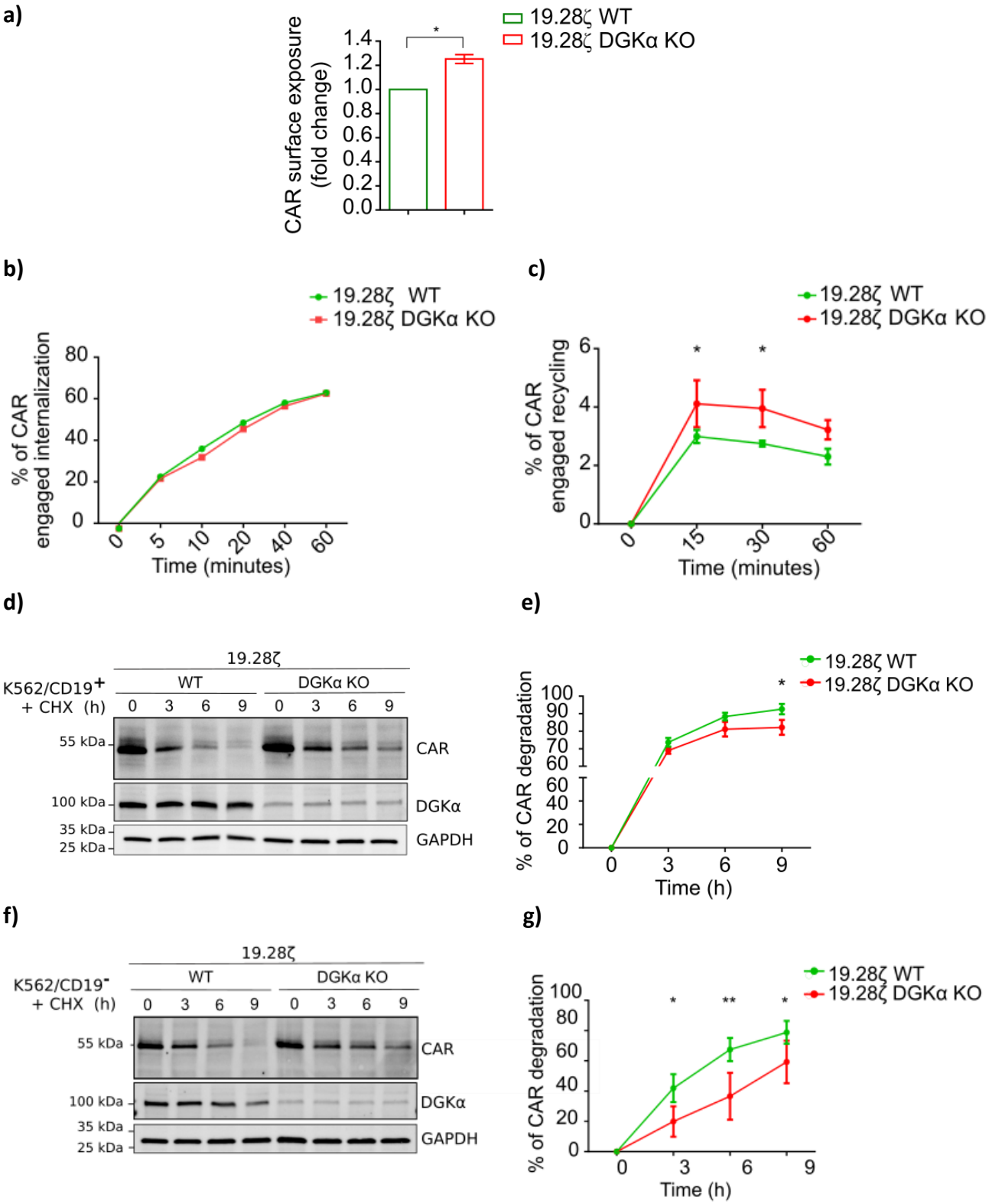

Figure 6. Engaged and basal CAR fate: (a) Quantification of total CAR at the cell surface by FACS analysis in 19.28ζ Jurkat WT and DGKα KO cell lines; paired t-test * p<0.05. **(b)** Percentage of engaged CAR internalized, n=1. **(c)** Percentage of CAR recycling after stimulation, n=3 independent experiment, data are presented as mean ± SEM; Two-Way ANOVA, Holm-Sidak's multiple comparisons test: * p < 0.05. (d,e) CAR degradation assay after treatment with CHX (100µg/ml) for the indicated time: **(d)** CAR expression was evaluated in 19.28ζ Jurkat WT and

DGKα KO co-incubated with K562/CD19+ by Western Blot analysis (left) and the quantification of degraded CAR is shown (right); **(e)** CAR expression in unstimulated condition (19.28ζ Jurkat co-incubated with K562/CD19-) analysed by Western Blot (left) and its relative quantification is shown (right); a small band was observed in DGKα KO due to the presence of K562,which physiologically contain DGKα.
Densitometry analysis of 3 independent experiments, Data are mean ± SEM; two-way ANOVA, Holm-Sidak's multiple comparisons test: * $p < 0.05$, ** $p < 0.01$.

CAR ubiquitination requires DGKα

Based on our results, we can speculate that DGKα limits the amount of CAR exposed to the cell surface primarily by promoting CAR degradation, which is a consequence of the ubiquitination of its CD3ζ chain (Li et al., 2020).

For this reason, we examined CAR ubiquitination by incubating or not 19.28ζ Jurkat cells with K562/CD19^{+} or CD19^{-} at 1:1 ratio for 5 minutes and, then CAR was immunoprecipitated in order to assess its ubiquitination level. Western blot analysis revealed an induction of ubiquitination in 19.28ζ WT cells when stimulated with the proper antigen, which was mirrored to a decrease in the amount of immunoprecipitated CAR (Fig.7a, b, c). However, in cells that were deleted for DGKα, CAR ubiquitination was significantly reduced, thus reflecting an impaired degradation (fig.7 a, b, c).

Among the mechanisms that controls receptor ubiquitination, the E3 ubiquitin ligase c-Cbl has been identified as the main regulator of CD3ζ degradation. Since CAR shares the CD3ζ chain with the TCR complex, we hypothesized that c-Cbl may also regulate CAR ubiquitination. Therefore, we performed a CAR immunoprecipitation analysis to examine the c-Cbl association with the CAR in our 19.28ζ Jurkat cells. Following stimulation, as confirmed by p-ERK1/2$^{T202/Y204}$ increasing level, c-Cbl co-immunoprecipitated with CAR in WT cells (Fig.7d, e). Then, we set to investigate whether DGKα could interfere with c-Cbl binding to the ζ chain of the receptor, thus affecting CAR loss. Interestingly, this association was reduced in stimulated 19.28ζ DGKα KO cells and partially rescued when we reintroduced both DGKA WT and KD (Fig.7d, e). Strikingly, DGKα itself was found to co-immunoprecipitate with the receptor in a stimulation-dependent manner, suggesting that may play a role in delivering c-Cbl to the CAR (Fig.7d, f).

Altogether, the data presented in this thesis demonstrate that DGKα recruits the E3 ubiquitin ligase c-Cbl to the receptor, thus increasing CAR ubiquitination, degradation and ultimately reducing the amount of the CAR at the cell surface. DGKα deletion restore CAR levels at the cell surface both in unstimulated and stimulated conditions by preventing tonic and antigen-induced degradation and promoting receptor recycling back to the plasma membrane. Together, these data contribute to the understanding of CAR-T cell functioning, providing a novel rationale to target DGKα in order to ameliorate CAR-T response rate.

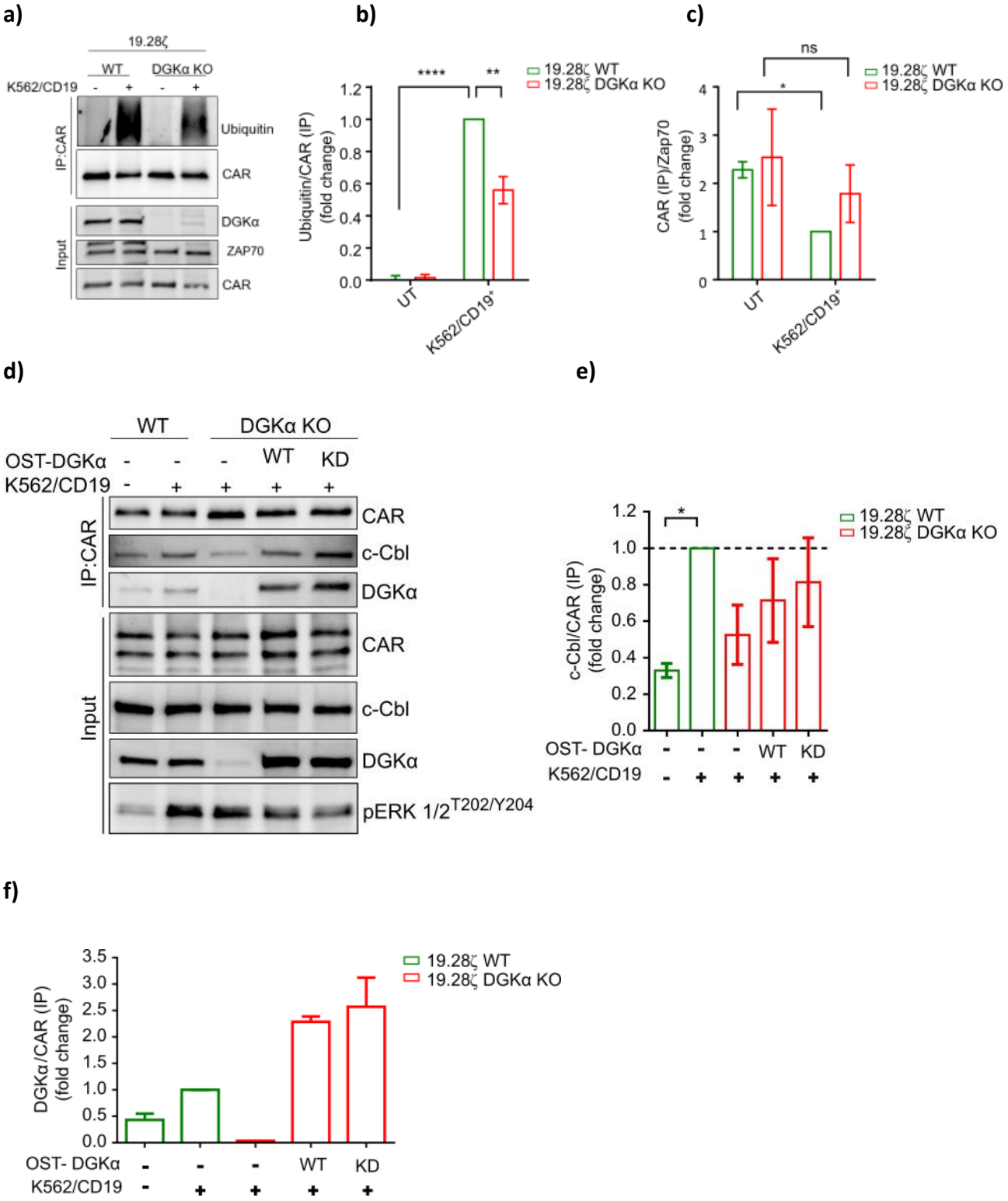

Figure 7. DGKα mediates CAR ubiquitination: (a) Representative blot of CAR immunoprecipitation in 19.28ζ Jurkat WT and DGKα KO cells under basal conditions (untreated, UT) or following engagement with K562/CD19^{+} cells. **(b)** Quantification of immunoprecipitated ubiquitin normalized on immunoprecipitated CAR level for each condition; n= 3 independent experiments, data are mean ± SEM; two-way ANOVA, Holm-Sidak's multiple comparisons test: ** $p < 0.01$, **** $p < 0.0001$. **(c)** Quantification of immunoprecipitated CAR on Zap70 in 19.28ζ Jurkat

WT and DGKα KO cells; n=4 independent experiments; data are mean ± SEM; two-way ANOVA, Sidak's multiple comparisons test: * $p < 0.05$. **(d)** Representative blot of CAR immunoprecipitation in 19.28ζ Jurkat cells co-incubated with K562/CD19^{+} or CD19^{-}. **(e)** Quantification of immunoprecipitated c-Cbl normalized on immunoprecipitated CAR level for each condition; n=3 independent experiments; data are mean ± SEM; one-way ANOVA, Sidak's multiple comparisons test: * $p < 0.05$. **(f)** Quantification of immunoprecipitated DGKα on immunoprecipitated CAR level for each cell line; n=2 independent experiments.

Discussion

CAR-T cell therapy represents a promising new frontier in cancer immunotherapy compared to classical chemotherapy, although it faces several limitations. These include the downmodulation of receptors following antigen exposure and the challenges posed by the immunosuppressive tumour microenvironment.

In this thesis, we investigated the role of DGKα in modulating CAR trafficking, focusing specifically on the mechanisms contributing to receptor downmodulation at the cell surface. We used a 19.28ζ Jurkat cell model to explore the receptor downregulation mechanism in presence (WT) or absence of DGKα (DGKα KO). Recent findings demonstrated that CAR undergoes rapid ubiquitination, internalization, and lysosomal degradation following antigen encounter (Li et al 2020). Our findings in 19.28ζ WT cells confirmed what has been documented in the literature. Intriguingly, in our DGKα KO CAR model, we observed significantly reduced CAR downregulation following tumour antigen ligation, indicating a potential for more effective long-term tumour eradication. The phenotype observed in DGKα deficient cells is lost when DGKα is re-overexpressed in 19.28ζ WT cells. Notably, OST-DGKα WT or KD significantly increases the percentage of surface receptor loss similar to 19.28ζ WT, suggesting that this mechanism may dependent on a scaffolding activity of the protein itself rather than on its kinase activity.

Previous studies from our laboratory have demonstrated the involvement of DGKα in receptor trafficking, as evidenced in ovarian carcinoma cells where DGKα drives integrin recycling (α5β1) and invasive behaviour by generating PA required to dock Rab11FIP1 recycling endosome to the plasma membrane (Rainero et al., 2012). DGKα role in trafficking is also supported by our unpublished data showing that DGKα inhibition rescues defective TCR recycling and surface expression in hypofunctional SAP-deficient T cells. Starting from the observation that DGKα KO cells display higher levels of CAR at the cell surface, we investigated processes that lead to the modulation of the receptor at the cell surface. These processes include internalization, recycling and degradation.

While we didn’t observe any differences in the internalization rate of CAR over time in 19.28ζ WT compared to DGKα KO cells, DGKα KO cells displayed significantly increased recycling. This seems to confer a protective effect against degradation through a mechanism that is dependent on DGKα. We may speculate that the increased recycling could be due to enhanced receptor dynamics, allowing for higher surface expression. Whether having more or less CAR at the cell

surface may confer an advantage in term of CAR-T cell function and in vivo persistence is under debate. On one hand, several studies provide support and demonstrate that a reduction of CAR on the surface is a crucial mechanism that drive CAR-T cells dysfunction (Davenport et al., 2015; Eyquem et al., 2017; Walker et al., 2017; Li et al., 2020; Agarwal et al., 2023). In particular, in the context of CAR ALK-BBz and CAR 19BBz, it has been observed that cells with low levels of surface CAR expression exhibit reduced cytokine production compared to cells with high CAR expression (Walker et al., 2017). Similarly, in a study by Guedan et co-authors, low levels of surface CAR significantly diminished their antitumor function in a xenograft pancreatic tumour model (Guedan et al., 2018). Therefore, one strategy to improve CAR-T cell function may be to increase CAR levels at the cell surface. Indeed, in the study by Li and colleagues, a mutated version of the CAR with increased recycling rate (and limited loss from the cell surface upon antigen stimulation) is sufficient to exhibit greater persistence in vivo of the CAR-T cells, which show better long-term killing capacity (Li et al., 2020). Altogether, these studies provide strong evidences that increasing CAR at the cell surface may be considered as a good strategy to improve CAR-T cells fitness. However, recent literature warns about the possibility of expressing the receptor at high levels in order to avoid tonic signalling, which is sufficient to induce ligand-independent early T cell exhaustion and limit antitumor potency (Long et al., 2015; Frigault et al., 2015). Since in DGKα-deficient CAR-T cells we observed a significant increase in CAR surface expression already at basal levels, we cannot rule out that our treatment may curtail CAR-T cell persistence in vivo.

The cellular model we exploit in this thesis (i.e. 19.28ζ Jurkat cells and antigen-expressing K562 myelogenous leukemia cells) has been highly advantageous to determine the mechanism through which DGKα may control CAR trafficking. However, we are aware that it has several limitations; one future prospect is to assess the impact of DGKα in trafficking in CAR-T manufacturer from primary T cells, because they offer a more clinically relevant model compared to cell lines. Moreover, the use of primary CAR-T cells allows to perform crucial assays such as degranulation assays, killing assay and chronic antigen exposure assay (CAE) which are needed to study CAR-T cell effector functions.

Mechanistically, in our model we demonstrate that the decreased degradation of CAR in DGKα KO cells is linked to reduced recruitment of Cbl to the CAR, resulting in decreased receptor ubiquitination. Accordingly, we would expect an increase in signalling after CAR stimulation in DGKα KO cells, while we didn't observe any changes in pERK levels compared to WT cells. Interestingly, also c-Cbl and Cbl-b double KO (dKO) T cells, despite inducing a significant increase of the TCR at the cell surface, do not display an enhanced signalling downstream TCR activation,

rather the signalling appears to be sustained over time (Naramura, M. et al., 2002). Based on the similarities of these two models (DGKα KO and Cbl dKO) we can speculate that DGKα KO cells may mirror these effects.

Our results identify a new kinase-independent function of DGKα in receptor regulation: this hypothesis is supported by several studies demonstrating that DGKζ, but not DGKα, is the main regulator of DAG-mediated signalling after TCR stimulation (Joshi et al., 2013; Guo, et al., 2008; Ávila-Flores et al., 2017); moreover, previous studies were mostly conducted upon pharmacologically inhibition of both DGKs or by deleting both isoforms, thus making difficult to discern between the distinct function of the two kinases. Therefore, we may speculate that DGKα genetic ablation might increase T cell function with a mechanism which is at least partially independent from DAG increase, and that DGKα and ζ specific targeting may have different outcomes. Interestingly, a first in human study in participants with advanced solid tumours is currently ongoing that aim to establish the safety and dosing of a new compound (GS-9911) that specifically degrades DGK alpha isoform. The result of this clinical trial will be available in 2026 and may help in dissecting DGKα specific functions (https://classic.clinicaltrials.gov/ct2/show/NCT06082960).

Besides DGKα and Cbl, another key negative regulator of TCR and immune tolerance is CD5, which has been shown to interact with DGKα (Mori et al., 2020). In peripheral T cells, the Cbl family associates with CD5 upon TCR activation (Voisinne et al., 2018), suggesting that DGKα might play a scaffolding role either in CD5 recruitment to the plasma membrane, or in facilitating Cbl recruitment to the receptor through CD5, thereby influencing its turnover and signalling dynamics. Whether this mechanism can be applied to the CAR need to be investigated, as well as the contribution of DGKα. Therefore, we are currently designing DGKα and CAR proteomic experiments, in order to clarify how DGKα regulates CAR trafficking.

Recent work from Carl June lab demonstrate that CTLA-4 deletion dramatically improve the response rate of CAR-T cells manufactured from patients with leukaemia that previously failed CAR-T cell treatment (Agarwal et al., 2023). However, CTLA-4 deficient cells are able to eradicate tumours only in low tumour burden conditions, when CAR at the cell surface is high; when mice are challenged with high tumour burden, CAR is lost from the cell surface, and CTLA-4 KO CAR-T cells failed to clear tumours (Agarwal et al., 2023), highlighting the strong positive correlation between CAR surface exposure and CAR-T cell anti-tumour activity in vivo. Based on these evidences, we can speculate that the combination of inhibitory receptors inhibition (i.e. CTLA-4) and DGKα genetic deletion will greatly improve CAR-T cell response and persistence in preclinical

model.

Altogether, the data presented in this thesis provide a novel rationale to target DGKα in order to ameliorate CAR-T response rate.

Materials and Methods

Generation of OST-DGKα WT and OST-DGKα KD constructs

The coding sequences for OST-DGKα WT and OST-DGKα KD inserts were designed based on mRNA transcript variant 3 of Homo sapiens diacylglycerol kinase alpha (DGKA) gene (NCBI Reference Sequence NM_001345.5), adding RsrII and SalI restriction enzyme sites in order to generate sticky ends and clone them in a recipient plasmid. Those inserts were synthesized in a pUC57-Mini vector (AmpR) by GenScript (Donor Plasmid).

Thus, enzymatic digestion was performed with the indicated enzymes and the reaction buffer Cut SMART 10X Buffer (New England Biolabs, NEB) for 1 h at 37°C. The digestion products were loaded onto a 0.8% agarose gel and, then, isolated using Monarch® DNA Gel Extraction Kit (New England Biolabs, NEB #T1020) and quantificated using NanoDrop2000.

The Recipient Plasmid (LV CD19-CAR.28ζ H (PGK) eGFP (mCMV), 9826 bp) is a lentiviral vector provided by Casucci laboratory. From this original vector, the sequence encoding for CD19-CAR.28ζ was removed through enzymatic digestions using RsrII and SalI restriction enzymes as mentioned before.

Subsequently, the digest Recipient Plasmid (50ng) was ligated (in ratio 3:1) with the previously isolated human DNA sequence of OST-DGKα WT or the mutated KD variant derived from the Donor Plasmid. The ligation reaction was performed overnight at 16°C by using the T4 DNA Ligase enzyme (Invitrogen, #15224017).

The whole ligation product was used to transform competent bacteria. At the end, some of the obtained colonies were screened by Sanger sequencing (Eurofins Genomics) using one primer on the vector (Recipient Plasmid) and the other one on the insert (OST-DGKα WT or KD) to verify the correct incorporation.

Primer	Forward	Reverse
OST-DGKα (WT/KD) INSERT	CTCTGAGGCTCTGCGGATT	AACAGTCTCAGGCCGATCTC
RECIPIENT PLASMID	GACCGAATCACCGACCTCTCT	GGGCCACAACTCCTCATAA

Cell culture

Jurkat (E6.1) and K562 cells were cultured in complete media (RPMI-1640, Euroclone) supplemented with 10% of fetal bovine serum (FBS), at 37 °C and 5 % CO_2.

Jurkat DGKα KO (E9, H2 clones) cells were previously generated in our laboratory from Jurkat (E6.1) cells, here indicated as Jurkat WT.

Jurkat WT and DGKα KO cells were stably transduced with the lentiviral vector containing 19.28ζ CAR sequence (LV CD19-CAR.28ζ H (PGK) eGFP (mCMV) from Casucci Laboratory). After 24 hours, 19.28ζ WT and 19.28ζ DGKα KO Jutkat cells just generated were transduced again with the Recipient Plasmid either empty or containing OST-DGKα WT or OST-DGKα KD sequences.

K562 cells were stably transduced with a lentiviral vector containing the ectopic domain of CD19 antigen provided by Casucci laboratory.

Every new Jurkat or K562 cell line generated (Fig. 4a and Fig. 4e) was sorted with Sony SH800 Cell Sorter.

Instead, 293T cells were cultured in complete Dulbecco's Modified Eagle's Medium (DMEM, Euroclone) supplemented with 10% FBS, at 37°C and 5% CO_2.

$0.45*10^6$ 293T cells were plated in 1.5 mL of complete DMEM in a 6 well plate for transient transfection of Recipient Plasmid (4 µg) with Lipofectamine 3000 (Invitrogen, #L3000150).

CAR mRNA expression assay

RNA was extracted from $5*10^6$ cells of each 19.28ζ WT and DGKα KO lines (empty, OST-DGKα WT and OST-DGKα KD) using TRIzol (Invitrogen, #15596018) and quantified by NanoDrop2000. Then, samples were digested with DNase at 37°C for 30 minutes, which was subsequentially inactivated by heating at 65°C and with 2mM EDTA. Next, 1µg of RNA was retrotranscribed into cDNA (complementary DNA) using the High-Capacity cDNA Reverse Transcription Kit (Thermo Fisher, #4368813).

The resulting cDNA was quantified using qPCR (Luna Universal qPCR Master Mix from New England Biolabs, NEB #M3003E) with the 7900HT Fast Real-Time PCR System. 18s r-RNA was used as housekeeping control.

Real-Time PCR system using the following couple of SYBR primers:

SYBR PROBE	Forward	Reverse
CAR	ACCGTGAAGCTGCTGATCTA	GTGTTGCCTTGCTGACAG AA
18S r-RNA	TAGAGGGACAAGTGGCGTTC	CGCTGAGCCAGTCAGTGT

CAR loss assay

0.15 * 10^6 19.28ζ Jurkat cells were plated in 150 µl of complete media (RPMI + 10% FBS) and co-incubated at a 1:1 ratio with K562/CD19^{+} or CD19^{-} cells for 1 hour at 37°C with 5% CO_2.

Then, cells were stained 1 hour on ice with saturating concentration of anti-Myc Tag antibody (9B11), conjugate with Alexa Fluor 647 fluorophore (Cell Signalling Technologies, #2233). After washing with PBS, CAR surface exposure was measured using FACSCelesta (BD Bioscience) and analysed with FlowJo Software.

The percentage of CAR loss resulted by subtracting the amount of receptor on the surface (%TS$^{K562/CD19-}$) under basal conditions (with K562/CD19^{-}) from the receptor remaining (%TS$^{K562/CD19+}$) on the surface after antigen exposure (with K562/CD19^{+}).

$$\% \text{ of CAR loss} = \%TS^{K562/CD19-} - \%TS^{K562/CD19+}$$

Engaged CAR internalization

0.15*10^{6} 19.28ζ Jurkat cells were resuspended in 50 µl of RPMI 0% FBS + 1% BSA for each experimental point and incubated for 30 minutes at 37 °C and 5 % CO_2 to equilibrate. After washing with PBS, the cells were incubated 1 hour on ice with the anti-Myc-tag antibody (9B11, Cell Signaling Technology, #2276) at saturating concentration (0.4 µg) in 50 µl of RPMI 0% FBS + 1% BSA (Bovine Serum Albumin) for each experimental point, to allow binding to the CAR exposed on the plasma membrane at that moment. After extensively washes with PBS, the cells were centrifuged at 300 g for 5 minutes and resuspended at the concentration of 0.15*10^{6} cells in 50 µl of RPMI 0% FBS + 1% BSA. Immediately, 50 µL (representative of the CAR Total Surface point) were transferred into a 96-well round-bottom plate, which was maintained on ice until the end of the experiment.

Subsequently, the remaining cells were incubated at 37°C for the indicated time (0, 5, 10, 20, 40 and 60 minutes) in order to promote CAR internalization and then transferred to the 96-well plate on ice. After washing with cold PBS, the cells in the plate were incubated with APC-647 anti-mouse secondary antibody diluted 1:500 in FACS Buffer (PBS supplemented with 2% FBS) for 30 minutes on ice. At the end, cells were washed again and the internalized receptor was measured using FACSCelesta (BD Bioscience) and analysed with FlowJo Software.

The percentage of receptor internalization was determined using the following calculation:

$$\% \text{ engaged internalized receptor} = \frac{[\text{MFI (Ts)} - \text{MFI (time}_{internalization}\ \text{X})]}{\text{MFI (Ts)}} \times 100$$

Where MFI is the Median of Fluorescence Intensity detected in Total Surface (Ts) and MFI (time X) is the MFI measured at each time point.

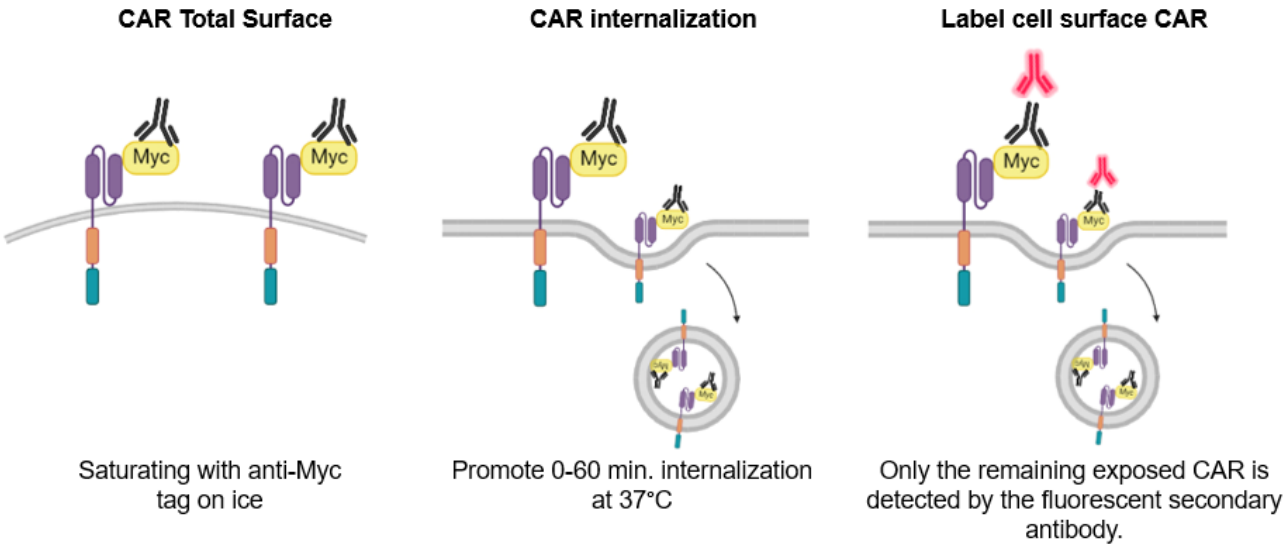

Figure 8. Engaged CAR internalization workflow: The cartoon illustrates the rationale of the engaged internalization experiment.

Engaged CAR recycling

As previous described for engaged CAR internalization, $0.15*10^6$ 19.28ζ Jurkat cells were resuspended in 50 µl of RPMI 0% FBS + 1% BSA for each experimental point and incubated 30 minutes at 37 °C 5 % CO_2. After washing with PBS, the whole CAR at the cell surface was coated with the anti-Myc-tag antibody (9B11, Cell Signaling Technology #2276) at a saturating concentration for 1 hour on ice.

Then, after two washes with PBS, cells were resuspended at the concentration of $0.15*10^6$ cells in 50 µl of RPMI 0% FBS + 1% BSA, and 50 µL representative of the CAR Total Surface point were directly transferred into a 96-well round-bottom plate on ice.

Then, the remaining cells were allowed to internalize the antibody-coated receptor for 20 minutes at 37°C and, at that time, 50 µL of cells were transferred in the 96-well plate on ice (20 minutes of internalization point). Thus, the remaining cells were treated for 30 seconds with Acid Stripping Solution (100 mM NaCl, 100 mM Glycine, 48.72 mM HCl, pH 2.5) in order to remove the anti-Myc-tag antibody bound to the receptor that is remained at the cell membrane, while internalized labelled CAR is protect from the stripping wash and preserve anti-Myc-tag antibody.

This reaction was stopped by washing twice with RPMI 0% FBS + 1% BSA and the cells were, finally, resuspended at the concentration of $0.15*10^6$ in 50 µl of the same media. Subsequently, 50 µl of cells were transferred in the 96-well plate to obtain the Stripped point (strip) that is representative of the time 0 (in which no signal should be present).

At this point, cells were incubated again at 37 °C to allowed labelled CAR recycling for the indicated time points (0, 15, 30 and 60 minutes) and transferred to the 96-well plate on ice. After washing with cold PBS, the cells were incubated with APC 647 anti-mouse secondary antibody diluted 1:500 in FACS Buffer for 30 minutes on ice.

After extensively washes, the recycled receptor was measured using FACSCelesta (BD Bioscience) and analysed with FlowJo Software.

The percentage of recycled receptor was determined using the following calculation:

$$\%\ \text{engaged recycled receptor} = \frac{[\text{MFI}\ (\text{time}_{recycling}) - \text{MFI}\ (\text{strip})]}{[\text{MFI}\ (\text{Ts}) - \text{MFI}(\text{strip})] - [\text{MFI}(\text{time}_{internalization}\ 20\text{min})] - \text{MFI}(\text{strip})]} \times 100$$

Where, MFI ($\text{Time}_{\text{recycling}}$) is the MFI detected at each recycling time points, MFI (strip) is the MFI measured at the Stripped point, MFI (TS) is the one measured at the Total Surface point and MFI ($\text{time}_{\text{internalization}}$20 min) is the MFI detectable after 20 minutes of internalization.

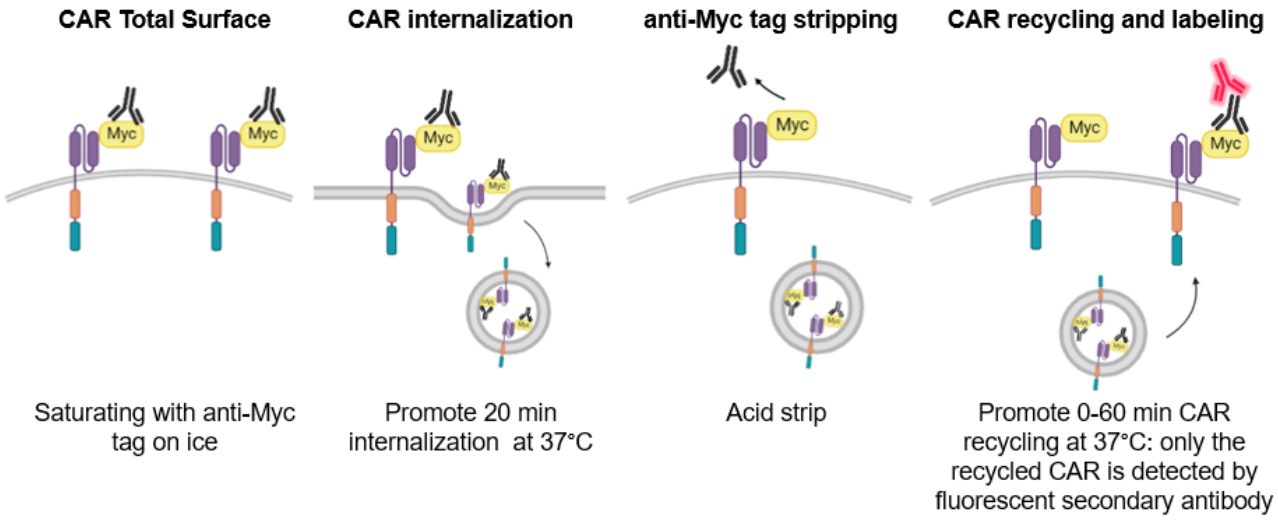

Figure 9. Engaged CAR recycling workflow: The cartoon illustrates the rationale of the engaged recycling experiment.

Degradation assay

$0.3*10^6$ 19.28ζ Jurkat cells were plated in 150 µl of RPMI 10% FBS medium for each experimental point in ratio 1:1 with K562/CD19$^+$ or CD19$^-$ cells in a 24 well-plate.

Cells were treated with CHX (100µg/ml) for 0, 3, 6, 9 hours and incubated at 37°C with 5 % CO2.

Then the cells were lysed in 70 µl of RIPA Lysis buffer (20 mM Tris-HCl pH 7.4, 160 mM NaCl, 50 mM NaF, 1 mM EGTA, 1 mM EDTA, 0.1% SDS, 0.1 % Sodium Deoxycholate, 1% TritonX-100) supplemented with Protease Inhibitor Cocktail (Sigma-Aldrich, #P8340). And 1mM Sodium Orthovanadate, for 30 minutes on ice.

At the end to purify the proteins from DNA, the lysed was centrifugated at 12000 g for 15 minutes at 4°C. In conclusion, proteins were denatured with Sample buffer (62.5 mM Tris-HCl pH 6.8, 10% Glycerol, 2% SDS) and 150 mM Dithiothreitol (DTT) and resolved by Western Blot.

CAR immunoprecipitation assay

$2*10^6$ 19.28ζ Jurkat cells were resuspended in 200 µl of RPMI 10% FBS in Eppendorf tubes and incubated in ratio 1:1 with K562/$CD19^+$ or $CD19^-$ cells for 5 minutes at 37°C.

Subsequently, the cells were lysed for 30 minutes on ice in 300 µl of Lysis Buffer containing 50 mM Tris-HCl (pH 7.6), 1% Triton X-100, 200 mM NaCl, 1 mM EDTA, 0.2% SDS, with the addition of freshly prepared 10 mM N-ethylmaleimide (Sigma Aldrich #04259-5G), Protease Inhibitor Cocktail (Sigma-Aldrich, #P8340) and 1mM Sodium Orthovanadate, 2 mM phenylmethylsulfonyl fluoride (PMSF) and 50 mM NaF. Then, proteins were purified from DNA by centrifugation at 12000 g for 15 minutes at 4°C.

Then, an equal amount of cell lysate (around 270 µl) was used to immunoprecipitate the CAR and the remaining part (around 30 µl) was kept as input for western blot analysis. For CAR immunoprecipitation, cell lysate was incubated with 15 µl of agarose beads conjugated with anti-Myc antibody (Sigma-Aldrich #A7470) for 1 hour at 4°C in agitation.

After intensively washing with Lysis Buffer to avoid non-specific binding, the CAR immunoprecipitated in complex with the beads was eluted in 15 µl of Sample Buffer plus 150 mM DTT. Finally, inputs were denatured as described before and both immunoprecipitates and inputs were resolved by western blot.

Western blotting

Protein lysates obtained from the previous assays were denatured as mentioned before and heated at 95°C. Subsequently, an equal amount of proteins was loaded and separated through SDS-PAGE (SDS-Polyacrylamide Gel Electrophoresis) using a 4-15% polyacrylamide precasted gel by BioRad. Following the electrophoresis run, the proteins in the gels were transferred using trans-blot Turbo RTA transfer kit (#1704273). Then, membranes were saturated for 1 hour at room

temperature with a 3% BSA solution in T-TBS (TBS with 0.25% Tween20) and 0.01% Sodium Azide before being probed with specific antibodies.

Primary antibodies against Myc-tag (9B11, Cell Signaling Technology #2276), DGKα (Proteintech 11547-1-AP), c-Cbl (D4E10; Cell Signaling Technology, #8447), Ubiquitin (P4D1; Cell Signaling Technology, 3936), β-ACTIN (8H10D10; Cell Signaling Technology, #3700), GAPDH (14C10, Cell Signaling #2118), Vinculin (Sigma Aldrich #V9264) and Phospho-p44/42 MAPK (Erk1/2) T202/Y204 (Cell Signaling Technology #8334) were used.

Those primary antibodies were diluted to a concentration of 1:1000 or 1:2000 in 3% BSA in T-TBS + 0.01% Sodium Azide and were incubated overnight at 4°C. To detect the bound antibodies, the appropriate HRP-conjugated secondary antibody (PerkinElmer) was used at 1:3000 in T-TBS and incubated for 1 hour at room temperature. Bands were visualized through ECL Plus Substrate (PerkinElmer), and the resulting images were captured using ChemidocTouch (BioRad). The quantification of the bands was carried out utilizing Image Lab software (Biorad).

Statistical analysis

The data are presented as mean ± SEM. Statistical analysis was performed using GraphPad PRISM software. It was determined by a Student T-test or when compare more than two groups a Oneway ANOVA or Two-way ANOVA (α=0.05) with Sidak's multiple comparison correction. * $p < 0.05$, ** $p < 0.01$, *** $p < 0.001$, **** $p < 0.0001$ or uncorrected Fisher's LSD test.

Acknowledgments

Firstly, I wish to thank immensely Prof. Graziani and Dr. Valeria Malacarne for the opportunity they gave me, for the patience, the support and the guidance. After all, the greatest inspiration was how much love they put into their work and the way they transmitted it to me.
Secondly, I would like to thank Sabrina, Giulia and Raluca, for their help and for the all amazing working experience we spent together.
Lastly, I wish to thank the laboratory staff, in particular Elia and Lorenza in which I could always rely on every step of the way.
In conclusion, I learned that everything mentioned above contributed to a healthy, professional and productive environment, which was crucial to my success and professional accomplishments.

References

1. Acconcia F, Sigismund S, Polo S. Ubiquitin in trafficking: the network at work. Exp Cell Res. 2009 May 15;315(9):1610-8. doi: 10.1016/j.yexcr.2008.10.014. Epub 2008 Oct 28. PMID: 19007773.
2. Arranz-Nicolás J, Ogando J, Soutar D, Arcos-Pérez R, Meraviglia-Crivelli D, Mañes S, Mérida I, Ávila-Flores A. Diacylglycerol kinase α inactivation is an integral component of the costimulatory pathway that amplifies TCR signals. Cancer Immunol Immunother. 2018 Jun;67(6):965-980. doi: 10.1007/s00262-018-2154-8. Epub 2018 Mar 23. PMID: 29572701.
3. Ávila-Flores A, Arranz-Nicolás J, Andrada E, Soutar D, Mérida I. Predominant contribution of DGKζ over DGKα in the control of PKC/PDK-1-regulated functions in T cells. Immunol Cell Biol. 2017 Jul;95(6):549-563. doi: 10.1038/icb.2017.7. Epub 2017 Feb 6. PMID: 28163304.
4. Baldanzi G, Pighingai A, Bettio V, Rainero E, Traini S, Chianale F, Porporato PE, Filigheddu N, Mesturini R, Song S, Schweighoffer T, Patrussi L, Baldari CT, Zhong XP, van Blitterswijk WJ, Sinigaglia F, Nichols KE, Rubio I, Parolini O, Graziani A. SAP-mediated inhibition of diacylglycerol kinase α regulates TCR-induced diacylglycerol signaling. J Immunol. 2011 Dec 1;187(11):5941-51.
5. Brownlie RJ, Zamoyska R. T cell receptor signalling networks: branched, diversified and bounded. Nat Rev Immunol. 2013 Apr;13(4):257-69. doi: 10.1038/nri3403. PMID: 23524462.
6. Chauveau A, Le Floc'h A, Bantilan NS, Koretzky GA, Huse M. Diacylglycerol kinase α establishes T cell polarity by shaping diacylglycerol accumulation at the immunological synapse. Sci Signal. 2014 Aug 26;7(340):ra82. doi: 10.1126/scisignal.2005287. PMID: 25161317; PMCID: PMC4993625.
7. Chiang YJ, Hodes RJ. Regulation of T cell development by c-Cbl: essential role of Lck. Int Immunol. 2015 May;27(5):245-51. doi: 10.1093/intimm/dxu105. Epub 2014 Dec 4. PMID: 25477210; PMCID: PMC4406264.
8. Cutrupi S, Baldanzi G, Gramaglia D, Maffè A, Schaap D, Giraudo E, van Blitterswijk W, Bussolino F, Comoglio PM, Graziani A. Src-mediated activation of alpha-diacylglycerol

kinase is required for hepatocyte growth factor-induced cell motility. EMBO J. 2000 Sep 1;19(17):4614-22. doi: 10.1093/emboj/19.17.4614. PMID: 10970854; PMCID: PMC302077.

9. Dong D, Zheng L, Lin J, Zhang B, Zhu Y, Li N, Xie S, Wang Y, Gao N, Huang Z. Structural basis of assembly of the human T cell receptor-CD3 complex. Nature. 2019 Sep;573(7775):546-552.

10. Dustin ML, Chakraborty AK, Shaw AS. Understanding the structure and function of the immunological synapse. Cold Spring Harb Perspect Biol. 2010 Oct;2(10):a002311. doi: 10.1101/cshperspect.a002311. Epub 2010 Sep 15. PMID: 20843980; PMCID: PMC2944359.

11. Evnouchidou I, Caillens V, Koumantou D, Saveanu L. The role of endocytic trafficking in antigen T cell receptor activation. Biomed J. 2022 Apr;45(2):310-320. doi: 10.1016/j.bj.2021.09.004. Epub 2021 Sep 28. PMID: 34592497; PMCID: PMC9250096.

12. Fu L, Li S, Xiao W, Yu K, Li S, Yuan S, Shen J, Dong X, Fang Z, Zhang J, Chen S, Li W, You H, Xia X, Kang T, Tan J, Chen G, Yang AK, Gao Y, Zhou P. DGKA Mediates Resistance to PD-1 Blockade. Cancer Immunol Res. 2021 Apr;9(4):371-385. doi: 10.1158/2326-6066.CIR-20-0216. Epub 2021 Feb 19. PMID: 33608256.

13. Gavali S, Liu J, Li X, Paolino M. Ubiquitination in T-Cell Activation and Checkpoint Inhibition: New Avenues for Targeted Cancer Immunotherapy. Int J Mol Sci. 2021 Oct 6;22(19):10800. doi: 10.3390/ijms221910800. PMID: 34639141; PMCID: PMC8509743.

14. Geisler C. TCR trafficking in resting and stimulated T cells. Crit Rev Immunol. 2004;24(1):67-86. doi: 10.1615/critrevimmunol.v24.i1.30. PMID: 14995914.

15. Guo R, Wan CK, Carpenter JH, Mousallem T, Boustany RM, Kuan CT, Burks AW, Zhong XP. Synergistic control of T cell development and tumor suppression by diacylglycerol kinase alpha and zeta. Proc Natl Acad Sci U S A. 2008 Aug 19;105(33):11909-14. doi: 10.1073/pnas.0711856105. Epub 2008 Aug 8. PMID: 18689679; PMCID: PMC2575297.

16. Jackson HJ, Rafiq S, Brentjens RJ. Driving CAR T-cells forward. Nat Rev Clin Oncol. 2016 Jun;13(6):370-83. doi: 10.1038/nrclinonc.2016.36. Epub 2016 Mar 22. PMID: 27000958; PMCID: PMC5529102.

17. Joshi RP, Schmidt AM, Das J, Pytel D, Riese MJ, Lester M, Diehl JA, Behrens EM, Kambayashi T, Koretzky GA. The ζ isoform of diacylglycerol kinase plays a predominant role in regulatory T cell development and TCR-mediated ras signaling. Sci Signal. 2013 Nov

26;6(303):ra102. doi: 10.1126/scisignal.2004373. PMID: 24280043; PMCID: PMC4096120.

18. June CH, O'Connor RS, Kawalekar OU, Ghassemi S, Milone MC. CAR T cell immunotherapy for human cancer. Science. 2018 Mar 23;359(6382):1361-1365. doi: 10.1126/science.aar6711. PMID: 29567707.

19. Jung IY, Kim YY, Yu HS, Lee M, Kim S, Lee J. CRISPR/Cas9-Mediated Knockout of DGK Improves Antitumor Activities of Human T Cells. Cancer Res. 2018 Aug 15;78(16):4692-4703. doi: 10.1158/0008-5472.CAN-18-0030. Epub 2018 Jul 2. PMID: 29967261.

20. Krishna S, Zhong X. Role of diacylglycerol kinases in T cell development and function. Crit Rev Immunol. 2013;33(2):97-118. doi: 10.1615/critrevimmunol.2013006696. PMID: 23582058; PMCID: PMC3689416.

21. Kureshi R, Bello E, Kureshi CTS, Walsh MJ, Lippert V, Hoffman MT, Dougan M, Longmire T, Wichroski M, Dougan SK. DGKα/ζ inhibition lowers the TCR affinity threshold and potentiates antitumor immunity. Sci Adv. 2023 Nov 24;9(47):eadk1853. doi: 10.1126/sciadv.adk1853. Epub 2023 Nov 24. PMID: 38000024; PMCID: PMC10672170.

22. Liu YC, Gu H. Cbl and Cbl-b in T-cell regulation. Trends Immunol. 2002 Mar;23(3):140-3. doi: 10.1016/s1471-4906(01)02157-3. PMID: 11864842.

23. Long AH, Haso WM, Shern JF, Wanhainen KM, Murgai M, Ingaramo M, Smith JP, Walker AJ, Kohler ME, Venkateshwara VR, Kaplan RN, Patterson GH, Fry TJ, Orentas RJ, Mackall CL. 4-1BB costimulation ameliorates T cell exhaustion induced by tonic signaling of chimeric antigen receptors. Nat Med. 2015 Jun;21(6):581-90. doi: 10.1038/nm.3838. Epub 2015 May 4. PMID: 25939063; PMCID: PMC4458184.

24. Mariuzza RA, Agnihotri P, Orban J. The structural basis of T-cell receptor (TCR) activation: An enduring enigma. J Biol Chem. 2020 Jan 24;295(4):914-925. doi: 10.1074/jbc.REV119.009411. Epub 2019 Dec 17. PMID: 31848223; PMCID: PMC6983839.

25. Martin-Salgado M, Ochoa-Echeverría A, Mérida I. Diacylglycerol kinases: A look into the future of immunotherapy. Adv Biol Regul. 2024 Jan;91:100999. doi: 10.1016/j.jbior.2023.100999. Epub 2023 Nov 2. PMID: 37949728.

26. Mérida I, Avila-Flores A, García J, Merino E, Almena M, Torres-Ayuso P. Diacylglycerol kinase alpha, from negative modulation of T cell activation to control of cancer progression. Adv Enzyme Regul. 2009;49(1):174-88. doi: 10.1016/j.advenzreg.2009.01.003. PMID: 19534031.

27. Merida I, Graziani A, Sakane F. Editorial: Diacylglycerol Kinase Signalling. Front Cell Dev

Biol. 2017 Sep 21;5:84. doi: 10.3389/fcell.2017.00084. PMID: 28983484; PMCID: PMC5613129.

28. Mori D, Grégoire C, Voisinne G, Celis-Gutierrez J, Aussel R, Girard L, Camus M, Marcellin M, Argenty J, Burlet-Schiltz O, Fiore F, Gonzalez de Peredo A, Malissen M, Roncagalli R, Malissen B. The T cell CD6 receptor operates a multitask signalosome with opposite functions in T cell activation. J Exp Med. 2021 Feb 1;218(2):e20201011. doi: 10.1084/jem.20201011. PMID: 33125054; PMCID: PMC7608068.

29. Olenchock BA, Guo R, Carpenter JH, Jordan M, Topham MK, Koretzky GA, Zhong XP. Disruption of diacylglycerol metabolism impairs the induction of T cell anergy. Nat Immunol. 2006 Nov;7(11):1174-81. doi: 10.1038/ni1400. Epub 2006 Oct 8. PMID: 17028587.

30. Onnis A, Baldari CT. Orchestration of Immunological Synapse Assembly by Vesicular Trafficking. Front Cell Dev Biol. 2019 Jul 3;7:110. doi: 10.3389/fcell.2019.00110. PMID: 31334230; PMCID: PMC6616304.

31. Prinz PU, Mendler AN, Masouris I, Durner L, Oberneder R, Noessner E. High DGK-α and disabled MAPK pathways cause dysfunction of human tumor-infiltrating CD8+ T cells that is reversible by pharmacologic intervention. J Immunol. 2012 Jun 15;188(12):5990-6000. doi: 10.4049/jimmunol.1103028. Epub 2012 May 9. PMID: 22573804.

32. Rainero E, Caswell PT, Muller PA, Grindlay J, McCaffrey MW, Zhang Q, Wakelam MJ, Vousden KH, Graziani A, Norman JC. Diacylglycerol kinase α controls RCP-dependent integrin trafficking to promote invasive migration. J Cell Biol. 2012 Jan 23;196(2):277-95. doi: 10.1083/jcb.201109112. PMID: 22270919; PMCID: PMC3265946.

33. Riese MJ, Wang LC, Moon EK, Joshi RP, Ranganathan A, June CH, Koretzky GA, Albelda SM. Enhanced effector responses in activated CD8+ T cells deficient in diacylglycerol kinases. Cancer Res. 2013 Jun 15;73(12):3566-77. doi: 10.1158/0008-5472.CAN-12-3874. Epub 2013 Apr 10. PMID: 23576561; PMCID: PMC3686869.

34. Ruffo E, Malacarne V, Larsen SE, Das R, Patrussi L, Wülfing C, Biskup C, Kapnick SM, Verbist K, Tedrick P, Schwartzberg PL, Baldari CT, Rubio I, Nichols KE, Snow AL, Baldanzi G, Graziani A. Inhibition of diacylglycerol kinase α restores restimulation-induced cell death and reduces immunopathology in XLP-1. Sci Transl Med. 2016 Jan 13;8(321):321ra7. doi: 10.1126/scitranslmed.aad1565. PMID: 26764158; PMCID: PMC4918505.

35. Shifrut E, Carnevale J, Tobin V, Roth TL, Woo JM, Bui CT, Li PJ, Diolaiti ME, Ashworth A,

Marson A. Genome-wide CRISPR Screens in Primary Human T Cells Reveal Key Regulators of Immune Function. Cell. 2018 Dec 13;175(7):1958-1971.e15. doi: 10.1016/j.cell.2018.10.024. Epub 2018 Nov 15. PMID: 30449619; PMCID: PMC6689405.

36. Smith-Garvin, J. E., Koretzky, G. A. & Jordan, M. S. T cell activation. Annual review of immunology 27, 591–619, doi:10.1146/annurev.immunol.021908.132706 (2009).

37. Sterner, R.C., Sterner, R.M. CAR-T cell therapy: current limitations and potential strategies. Blood Cancer J. 11, 69 (2021). https://doi.org/10.1038/s41408-021-00459-7

38. Wu L, Wei Q, Brzostek J, Gascoigne NRJ. Signaling from T cell receptors (TCRs) and chimeric antigen receptors (CARs) on T cells. Cell Mol Immunol. 2020 Jun;17(6):600-612. doi: 10.1038/s41423-020-0470-3. Epub 2020 May 25. PMID: 32451454; PMCID: PMC7264185.

39. Zhou P, Shaffer DR, Alvarez Arias DA, Nakazaki Y, Pos W, Torres AJ, Cremasco V, Dougan SK, Cowley GS, Elpek K, Brogdon J, Lamb J, Turley SJ, Ploegh HL, Root DE, Love JC, Dranoff G, Hacohen N, Cantor H, Wucherpfennig KW. In vivo discovery of immunotherapy targets in the tumour microenvironment. Nature. 2014 Feb 6;506(7486):52-7. doi: 10.1038/nature12988. Epub 2014 Jan 29. PMID: 24476824; PMCID: PMC4052214.